WELDING RESEARCH

SUPPLEMENT TO THE *WELDING JOURNAL*, JUNE 1999

Sponsored by the American Welding Society and the Welding Research Council

Determination of Mechanical and Fracture Properties of Laser Beam Welded Steel Joints

Flat microtensile specimens were found suitable for determining the mechanical properties of similar and dissimilar laser beamweld joints

BY G. ÇAM, S. ERIM, Ç. YENI AND M. KOÇAK

ABSTRACT. Laser beam (LB) welding is increasingly being used in welding of structural steels. The thermal cycles associated with laser beam welding are generally much faster than those involved in conventional arc welding processes, leading to a rather small weld zone, that usually exhibits a high hardness for C-Mn structural steels due to the formation of martensite. It is rather difficult to determine the tensile properties of a laser weld joint area due to the small size of the fusion zone. Complete information on the tensile and fracture toughness properties of the fusion zone is essential for prequalification and a complete understanding of the joint performance in service, as well as for conducting the defect assessment procedure for such weld joints. Therefore, an experimental investigation on the mechanical properties of laser welded joints using flat microtensile specimens (0.5 mm thick, 2 mm wide) was carried out to establish a testing procedure to determine the tensile properties of the weld metal and heat-affected zone (HAZ) of the laser beam welds.

In the present work, two similar joints, namely, ferritic-ferritic and austenitic-austenitic and one dissimilar ferritic-austenitic joint were produced with a CO_2 laser using 6-mm-thick steel plates. In addition to the testing of flat microtensile specimens, the mechanical properties were examined by microhardness survey and conventional transverse and round tensile specimens. The results of the microtensile specimens were compared with standard round tensile specimens, and this clearly showed the suitability of the microtensile specimen technique for such joints. The crack tip opening displacement (CTOD) tests were also performed to determine the fracture toughness of the LB welds using three-point bend specimens. The effect of strength heterogeneity (mismatching) across the weld joint and at the vicinity of the crack tip on the CTOD fracture toughness values was also discussed.

Introduction

Steel is a good absorber of the light wave lengths produced by CO_2 and Nd:YAG lasers and many steels are readily weldable by this process. A series of studies describing the successful use of laser beam (LB) welding to different steels in various industrial applications can be found in the literature (Refs. 1–9). However, the chemical composition (particularly C, P and S contents as well as carbon equivalent) of the structural steels significantly influences the laser weldability of these materials. In modern structural steels, the carbon content is significantly reduced and the strength is attained by alloying elements and/or thermal processing during rolling. These fine-grained steels are particularly suitable for the low-heat-input laser welding process to avoid the development of a coarse-grained microstructure in the HAZ region. However, the low heat input and high cooling rate (high welding speed) typical of this process promote the formation of hard and brittle microstructures (*i.e.,* martensite) within the narrow weld and HAZ regions of steels subjected to solid-state phase transformations. Since the hardness values reached in these regions are usually well above those specified in standards and codes of conventional arc welds, expensive and time-consuming qualification procedures may be required for some components (Ref. 10). It has been reported (Ref. 11) that the use of the IIW formula for carbon equivalent (C_{eq}) is not adequate to assess the hardening effect in the fusion zone of the laser welds of C-Mn steels.

The weld formation and quality of LB steel weldments are usually associated with three aspects: porosity, solidifica-

KEY WORDS

Laser Beam Welding
LBW
CO_2 Laser
Fracture Toughness
Flat Microtensile
Hardness Test
Crack Tip Opening
C-Mn Steel
HAZ

G. ÇAM and M. KOÇAK are with GKSS Research Center, Institute of Materials Research, Geesthacht, Germany. S. ERIM and Ç. YENI are with Dokuz Eylül University, Mechanical Engineering Dept., Izmir, Turkey.

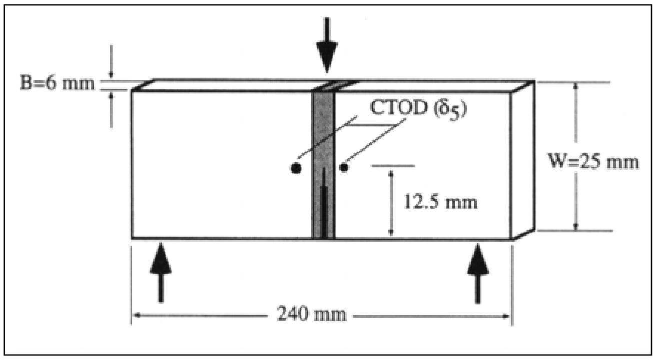

Fig. 1 — Three-point bend specimen geometry for fracture toughness testing.

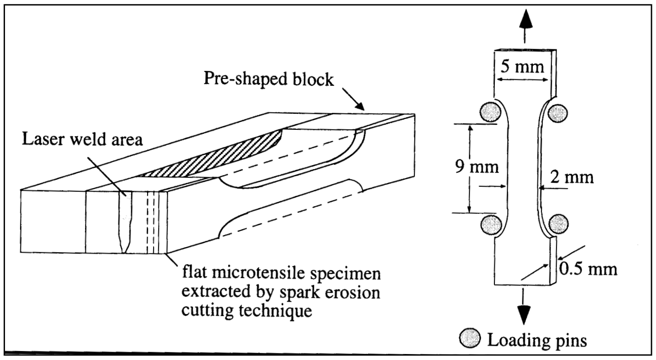

Fig. 2 — Schematic showing the extraction and loading of the flat microtensile specimens.

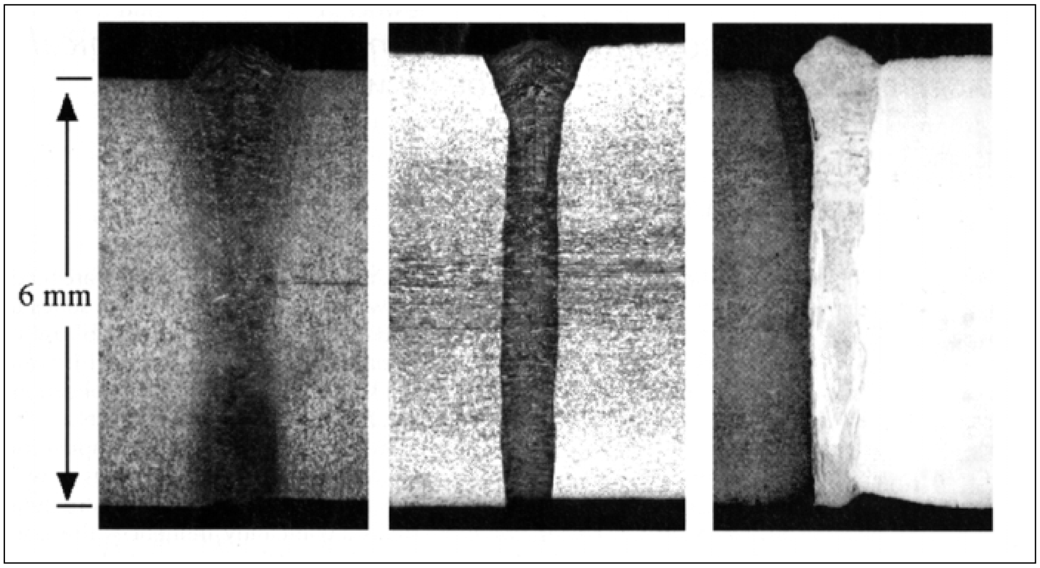

Fig. 3 — Macrosections of the joints. A — Similar ferritic; B — similar austenitic; C — dissimilar joints.

tion cracking and high hardness in the HAZ and fusion zone. Pores are formed as a result of dissolved gases or gases arising from contaminated surfaces, trapped process gases or evaporation of alloying elements. In the case of steels, porosity has been in general associated with low grade rimmed steels with oxygen contents above 100 ppm especially as thin sheet material, although the literature also reports this type of discontinuities on weldments produced in higher steel grades (Ref. 5). At excessive weld cooling rates, the rate of escape of bubbles eventually formed in the fusion zone can be lower than the rate of solidification resulting in various degrees of porosity in the final weld. A recent study (Ref. 5) on different steel grades, thickness and welding speeds have shown that generally the porosity level associated with slower welds is higher than those connected with faster welding speeds. The evaluation of the weldment quality may, however, reveal that higher porosity levels, irrespective of base plate type, do not have a particularly detrimental effect on weld joint transverse tensile properties due to high strength overmatching of the fusion zone, which effectively shields the defective weld zone.

There are no fracture mechanics based fracture toughness testing procedures available for laser beam weld ed joints despite the wide and inevitable use in modern engineering structures. This discrepancy is due mainly to the lack of information on the interaction between the base metal and fusion zone, which have significantly different tensile properties. Substantial differences in strength properties (mismatching) of the base metal and narrow fusion zone of the LB welds inevitably occur due to the rapid thermal cycle of the joining process. For the CTOD toughness determination, the effects of specimen geometry (*e.g.* weld width, crack size, notch position, etc.) and the degree of strength mismatch (mismatch ratio, M = yield strength of fusion zone/yield strength of base plate) between base metal and weld zone on toughness have, therefore, to be taken into account (Refs. 12–17).

Almost all LB welded structural C-Mn steels exhibit a weld metal region of higher hardness and strength (possibly with lower toughness) compared to the base metal (overmatching) due to the rapid solidification and single pass nature of the welding process. The laser weld region with its high hardness and strength makes it almost impossible to determine the "intrinsic fracture toughness" properties of the weld region using conventional Charpy-V notch impact (Ref. 18) and CTOD toughness (Ref. 2) testing specimens due to the crack path deviation towards the softer base metal as a result of mechanical property mismatch between the base metal and the weld zone. Therefore, both test results can only provide information on the toughness performance of the whole joint under impact and static bending loading conditions. They cannot provide required intrinsic toughness properties of the fusion zone due to inevitable interaction between weld zone and base plate. The toughness result obtained from such a specimen will inevitably be higher due to tougher base metal, but the result should not necessarily be classified as an "invalid" toughness result. An inevitable interaction between lower strength base metal (at a distance of about 1.5 mm to the crack tip) and the crack tip will occur and hence relax the stress-state (*i.e.* constraint) at the crack tip. Plasticity development in the base metal will subsequently prevent the brittle fracture initiation in the laser beam weld zone, which contains a martensitic microstructure and hence high hardness. The fracture toughness testing procedure for LBW joints should take this very natural phenomenon into account and hence should not take any artificial measure (by producing larger weld zone or extensive side-grooving) to force the fracture process to remain within the weld zone. This may be achieved in laboratory scale specimens, but fracture behavior of LBW joints will follow its own natural course during the service.

In the present study, an emphasis has also been given to the establishment of the flat microtensile specimen testing procedure and hence the determination of the tensile property gradient existing in the LB fusion zone. The flat microtensile specimen technique was originally developed for property determination of HAZ for conventional multipass weld joints (Ref. 19). Successful applications of this technique for thick-section similar and dissimilar electron beam welds (Ref. 12) and for the strength determination of diffusion welded joints (Refs. 20, 21) were also carried out at the GKSS research center. This study is an extension of these experimental activities and specifically addresses the development and refinement of the testing procedure for laser beam steel welds, and hence, similar and dissimilar laser beam weld joints between ferritic and austenitic steels produced by CO_2 laser using 6-mm thick plates were systematically investigated.

Experimental Procedure

In this study, austenitic stainless steel (grade 1.4404) and ferritic steel (grade St37) were used as base plates. The mechanical properties of the base plates are given in Table 1. Similar and dissimilar single-pass full penetration CO_2 LB welds on butt joints were produced without using filler metal. Extensive microhardness measurements (using 100-g load) were performed across the weld regions at three different locations, namely at the weld root, mid-section and top part of the joints. In addition, the HAZ region of the ferritic steel was also screened by conducting microhardness measurements parallel to the weld interface.

Nonstandard three-point bend specimens, which were machine notched in the weld zone, were further fatigue precracked in order to introduce a sharp crack (a/W = 0.5) as illustrated in Fig. 1, and they were tested at both room temperature and –40°C (–40°F). CTOD measurements using the GKSS developed d_5 clip gauges (Refs. 14, 22) were conducted on SENB specimens, which allowed a direct measurement of the crack tip opening displacement for each specimen.

Standard flat transverse-tensile specimens were extracted from the welded plates. Weld reinforcement was ma-

Table 1 — Base Metal Mechanical Properties Determined Using Standard Round Tensile Specimens

Base Material	YS (MPa)	TS (MPa)	Elongation %	Reduction in Area
St 37 (Ferritic)	233	368	36	51.06
1.4404 (Austenitic)	308	626	69	49.61

Mismatch ratio = M = YS_{St37}/YS_{aus} = 233/308 = 0.76

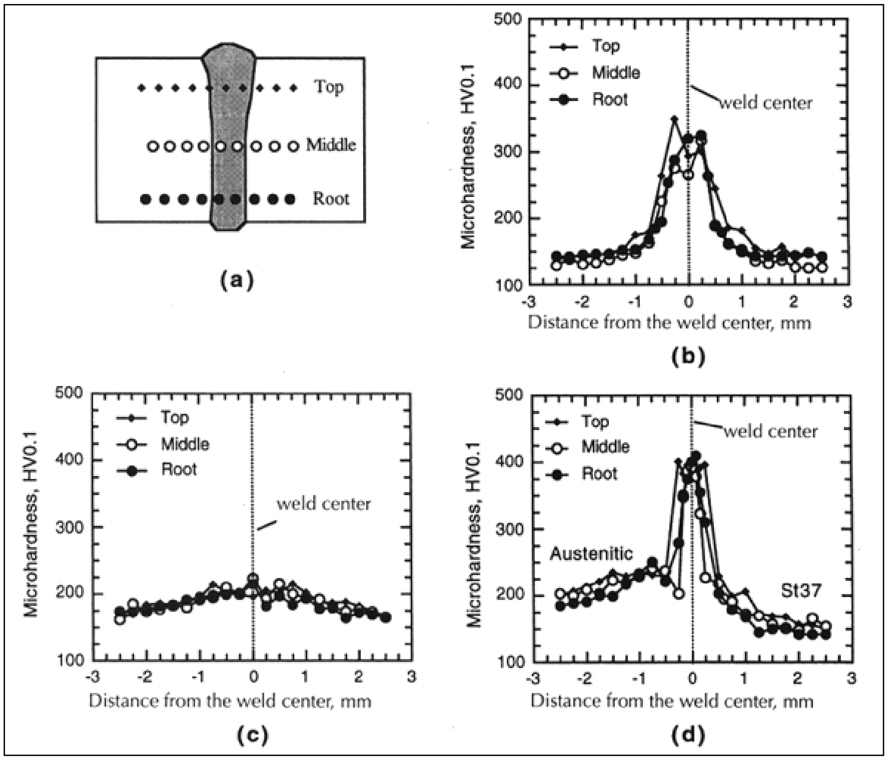

Fig. 4 — Hardness profiles of the joints. A — Schematic illustration of the micro-hardness measurement procedure; B — similar ferritic; C — similar austenitic; D — dissimilar joints.

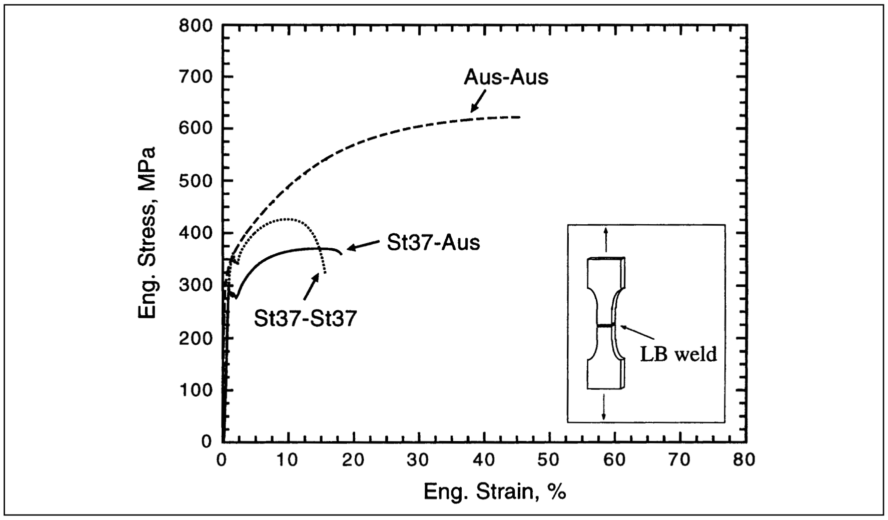

Fig. 5 — Stress-strain curves of LB weld joints determined by testing transverse tensile specimens.

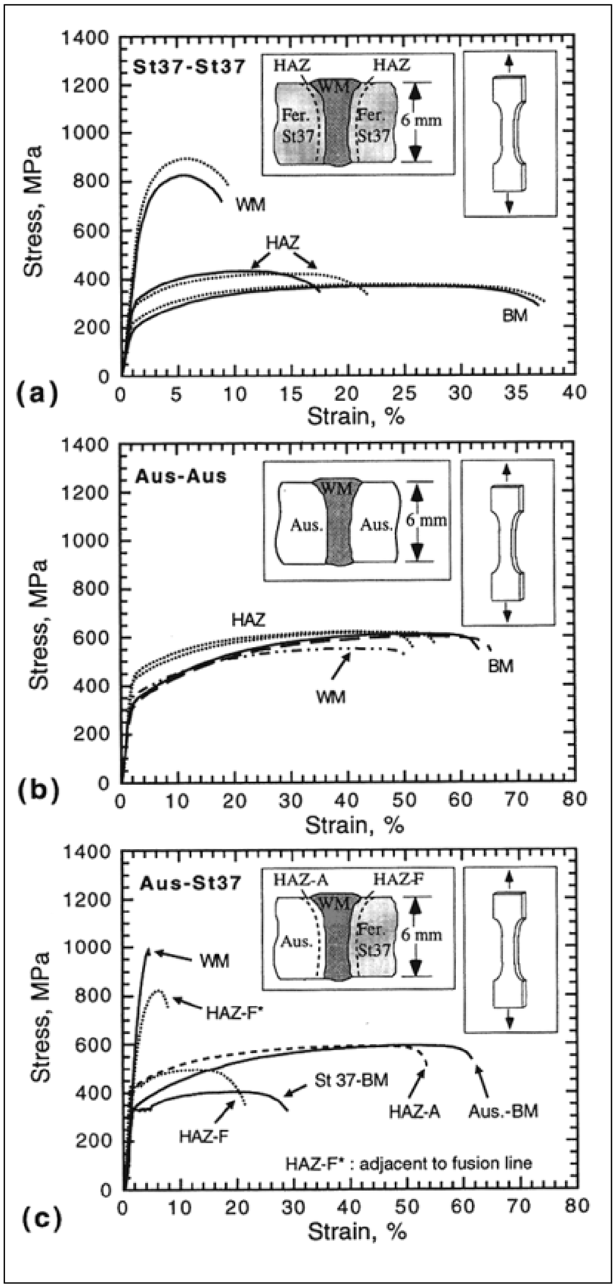

Fig. 6 — Stress-strain curves of the flat microtensile specimens extracted from: A — Similar ferritic; B — similar austenitic; C — dissimilar joints.

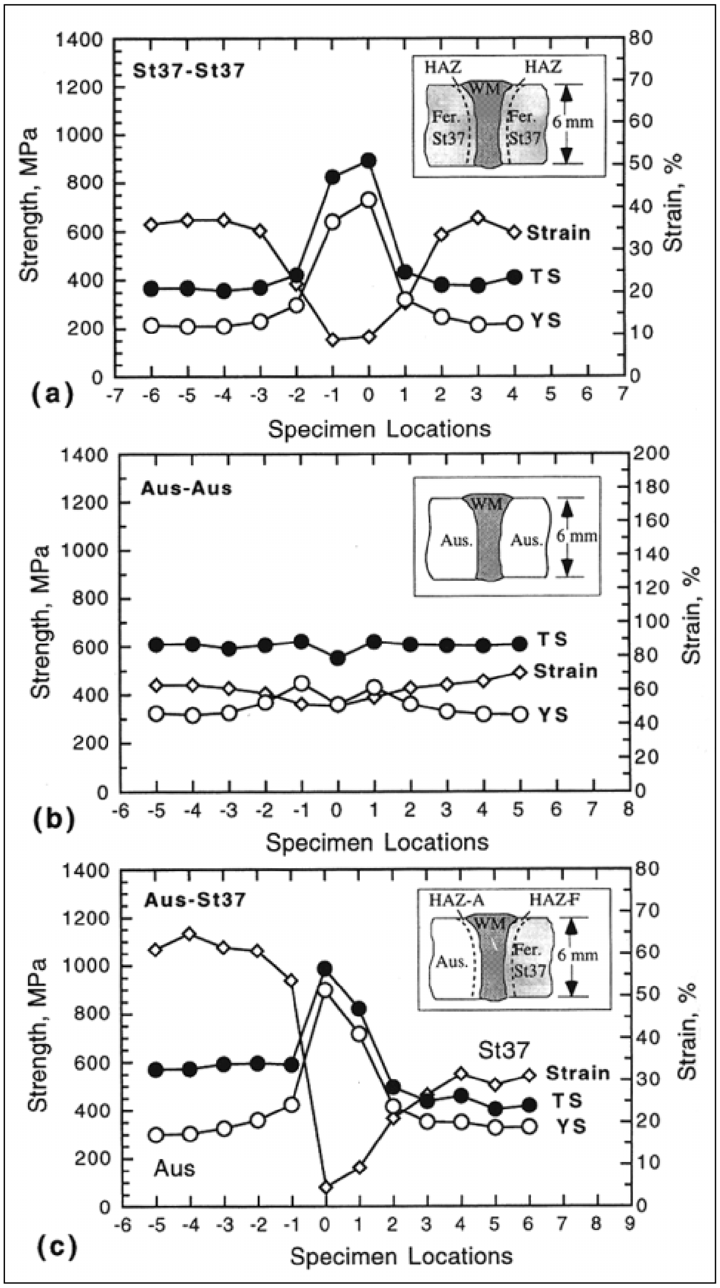

Fig. 7 — Mechanical property variations across the joints (0 represents the weld center): A — Similar ferritic; B — similar austenitic; C — dissimilar joints.

chined before testing. Sets of flat microtensile specimens were also extracted by spark erosion cutting from base metals, HAZs and weld metals of all the joints studied as schematically shown in Fig. 2. The flat microtensile specimen preparation was conducted mainly in two stages: 1) extraction of a pre-shaped block with laser weld in the middle, 2) cutting out specimens from etched pre-shaped block using a spark erosion cutting technique (with 0.1-mm diameter Cu wire) parallel to the weld. Due to the small size of the microtensile specimens, loading was introduced using four high-strength round pins at the shoulders of the specimens — Fig. 2. All tensile tests were carried out at room temperature using a displacement rate of 0.5 mm/min in a screw-driven universal testing machine. After testing, the broken half of the flat microtensile specimens were mounted for microstructural verification of the specimen location. The fracture surfaces of selected bend and tensile specimens were also examined by scanning electron microscopy for presence of porosity.

Results and Discussion

Microstructural Observations

Microstructural examinations of the joints investigated showed that the weld regions of similar ferritic and dissimilar joints contained bainite and martensite. Figure 3 shows macrosections of the joints. Similar ferritic joints displayed a weld metal structure consisting of bainite and martensite, whereas similar austenitic welds exhibited an austenite-dendritic (cellular) structure with no evidence of martensitic formation as expected. Contrary to a similar austenitic joint, a distinct HAZ development occurred in a similar ferritic joint. The HAZ in these joints contained a refined ferrite/pearlite structure and pearlite dissolution at the base metal sides. A dissimilar joint, on the other hand, showed an inhomogeneous weld metal microstructure containing a mixture of ferrite and austenite solidification structures in varying degrees due to an incomplete mixture of the molten metals of both sides in the weld pool during solidification. As reported earlier for dissimilar LB joints between St37 and austenitic steels (Refs. 2, 4), some solidification cracks parallel to the dendritic growth were observed in the weld zone of the dissimilar joints, which indicates that sufficient thermal stresses were developed in these weldments to separate the grain boundaries in the cellular structure during solidification, which was coarser than that in the weld metal of similar austenitic joints. The microstructural aspects of these joints were discussed in more detail in an earlier publication (Ref. 4).

Hardness

In order to determine the hardness profiles, extensive microhardness measurements were conducted at three positions (top, middle and root), Fig. 4A. The microhardness results exhibited no significant difference between these positions for all the weld joints studied, Fig. 4, implying that no significant gradient in mechanical properties of laser welds along the plate thickness direction is present. Similar ferritic steel joints displayed a high hardness profile in the weld region while austenitic welds showed almost no change in hardness across the joint. Similar St37 joints exhibited a peak hardness value of about 330 HV, whereas similar austenitic joints displayed a hardness value of about 210 HV in the weld region — Figs. 4B and 4C, respectively. This is expected due to the lack of bainite and/or martensite formation in the weld regions of austenitic joints. Dissimilar joints displayed a hardness peak of about 380–400 HV within the weld metal — Fig. 4D, which is slightly higher than that of similar ferritic weld metal.

Tensile Properties

Standard round tensile specimens from the base metal were tested to find out the strength mismatch ratio (M) as given in Table 1. The yield strength mismatch ratio, M = YS_{St37} / $YS_{1.4404}$, between the two base metals is found to be 0.76. Flat transverse tensile specimens were also tested to find out the nominal mechanical properties of the joints. The specimens of similar and dissimilar joints containing ferritic steel always failed in the lower strength ferritic base metal. The stress-strain curves obtained from flat transverse tensile specimens show some differences compared to the round tensile specimens due to the presence of LB weld region at the middle of the specimens. The stress-strain curve obtained from the flat transverse tensile specimens of the dissimilar joint lies between those of the similar joints of the constituent steels, as expected — Fig. 5. Evidently, these tests, particularly for ferritic joints where a high hardness profile exists, do not give any information on the local mechanical properties of the weld region.

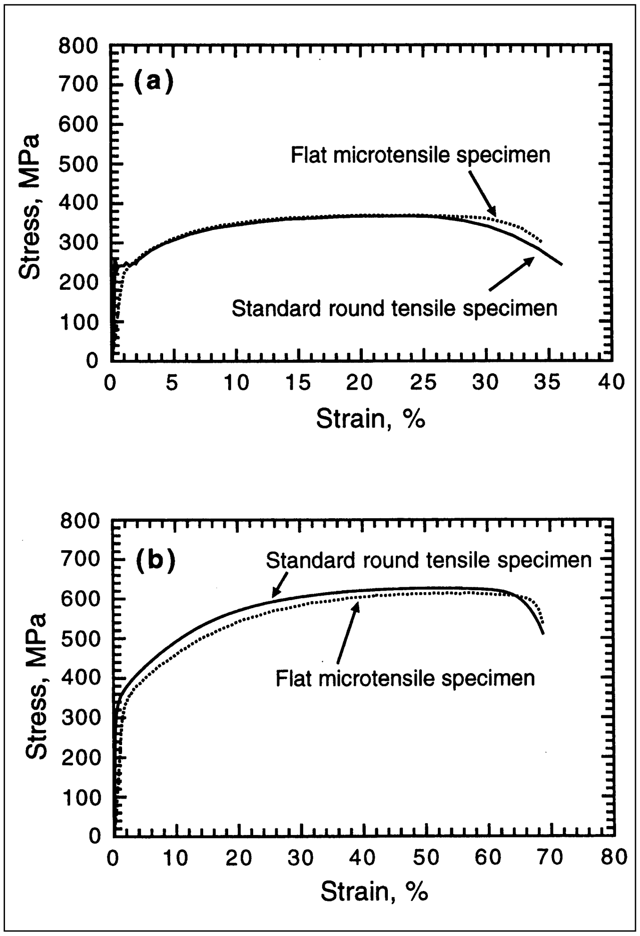

Fig. 8 — Comparison of the stress-strain curves of base metals obtained by testing standard round and flat microtensile specimens: A — Ferritic; B — austenitic steel.

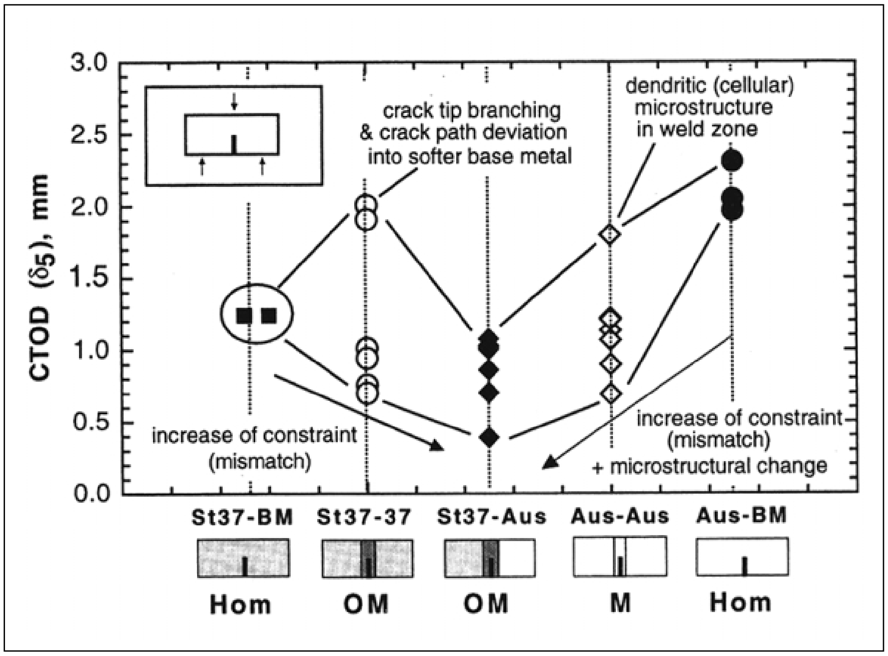

Fig. 9 — Comparison of CTOD values of base metals and laser beam welded joints at room temperature. Dissimilar joints exhibit lower toughness levels due to strength mismatch induced constraint at the crack tip. (Note: a different symbol has been used for each specimen configuration for clearness).

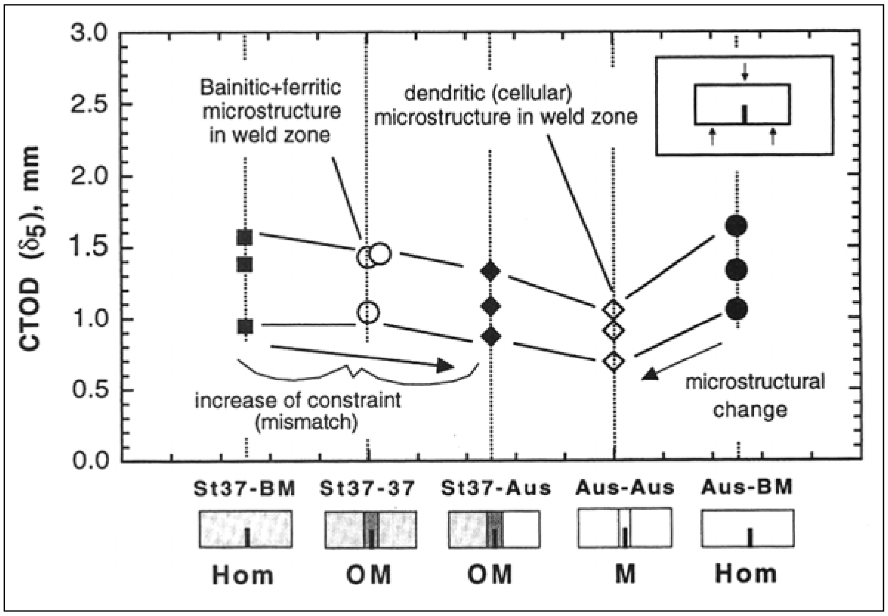

Fig. 10 — Comparison of CTOD values of base metals and laser beam welded joints at –40°C. (Note: a different symbol has been used for each specimen configuration for clearness).

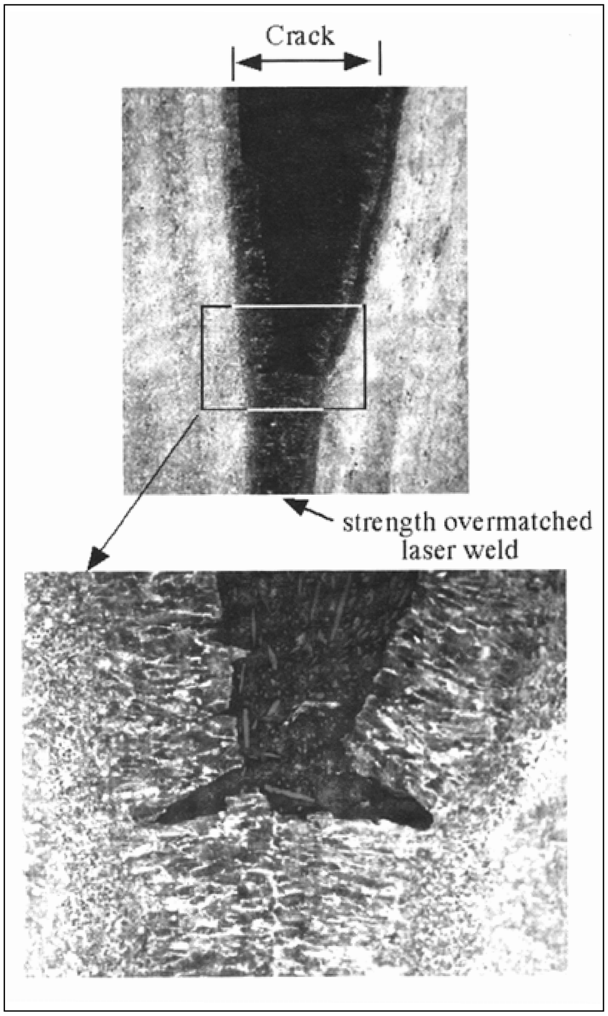

Fig. 11 — Crack tip branching and distinct crack path deviation into lower strength base metal in similar ferritic joint.

Therefore, all-weld metal and all-HAZ flat microtensile specimens were prepared and tested to determine the local mechanical properties of the respective areas in the weld regions. Table 2 summarizes the mechanical properties of the ferritic base metal (BM-F), austenitic base metal (BM-A), weld metal (WM), HAZ of ferritic steel (HAZ-F) and HAZ of austenitic steel (HAZ-A) on similar and dissimilar joints determined using microtensile specimens. The ferritic weld metal region exhibits the highest strength with approximately 310% strength overmatching as microhardness results indicated. The full stress-strain curves of these specimens are given in Fig. 6. The individual values of the yield strength (YS), tensile strength (TS) and fracture strain with respect to the specimen location are presented in Fig. 7.

Similar ferritic joint. Figure 6A illustrates the stress-strain curves of the microtensile specimens extracted from a similar ferritic joint, and Fig. 7A shows the variation in the mechanical properties of the same joint. As seen from these figures, the weld metal exhibits the highest strength level (overmatching, M = 3.1) and the lowest strain value compared to the BM and HAZ regions.

Similar austenitic joint. For the similar austenitic joint, the weld metal and HAZ exhibit slightly lower strain values with approximately 110% overmatching (Table 2) in the strength level — Figs. 6B and 7B.

Dissimilar joint. In the dissimilar joint, the weld metal exhibits a high strength level with a limited strain value as seen in Figs. 6C and 7C. The HAZ at the ferritic side (HAZ-F) also displays relatively higher strength levels and lower strain values than the ferritic base metal. The HAZ at the austenitic side (HAZ-A), on the other hand, does not exhibit a significant increase in strength, but some decrease in strain value as compared to austenitic base metal.

In order to investigate the suitability of microtensile specimen technique to determine the mechanical properties of laser beam welded joints, the stress-strain curves obtained from base metal microtensile specimens were compared with those obtained from base metal standard round tensile specimens — Fig. 8. As seen from this figure, microtensile specimens of the base metals exhibited similar stress-strain curves to those of standard round tensile specimens of the base metals, indicating that this technique can be successfully employed to determine the local mechanical properties of laser beam welded joints.

As demonstrated above, the mechanical properties (including full stress-strain curves) of each zone of laser beam welded similar and dissimilar joints can be successfully determined using flat microtensile specimens. Complete information (not only hardness values) on the local mechanical properties of laser welds is often essential for optimization of the laser welding process and filler metal development for various alloys, as well as quality control and fracture analyses (experimental and numerical) of the welds. Development of filler metal composition to reduce the hardenability of C-Mn steel joints and the softening of Al-alloy weld joints is currently of great interest. In order to make a step forward in these areas, complete information on the local properties of real weld joints should be generated. The tensile testing technique described in this paper can provide such information.

CTOD Fracture Toughness

The problem of measuring an "intrinsic fracture toughness" value (in terms of standardized CTOD or J) of mis-matched laser weld specimens is very hard to overcome due to the high strength mismatch within a very small region at the vicinity of the crack tip. It is not a simple task to distinguish the contributions from both the base metal (lower strength) and the narrow LB weld (highly overmatched) at the vicinity of the crack tip to the remotely measured crack mouth opening displacement (CMOD) and load line displacement (V_{LL}) usually used in standardized CTOD and J estimates.

A local and direct measurement technique (d_5 technique) was developed at GKSS Research Center as a measure of the CTOD for determining the fracture toughness and the crack growth resistance. It consists of measuring the relative displacement of two gauge points directly at the crack tip using special displacement gauges. The resulting CTOD is called d_5 because the gauge length over which the CTOD is determined amounts to 5 mm. The advantage of this measurement concept is that the d_5 type CTOD can be easily measured on any configuration with a surface breaking crack; no calibration functions are required. Another appealing aspect of the d_5 technique is that since it is measured locally as a displacement at the location of interest, it does not have to be inferred from remotely measured quantities, like the J integral or the standardized CTOD. This is of particular importance when the specimen is mechanically inhomogeneous, as is the case for highly mismatched strength in narrow laser welds. The CTOD values of the laser weld joints on the SENB specimens have, therefore, been measured in terms of the CTOD (d_5) technique.

For each weld condition, three deeply notched (a/W = 0.5) three-point bend specimens were tested at room temperature (RT) and –40°C, and they all exhibited fully ductile fracture behavior. Ferritic base metal displayed similar CTOD values at both testing temperatures, indicating that –40°C lies at the upper shelf of ductile-brittle transition for this ferritic steel grade, whereas austenitic base metal exhibited slightly lower CTOD values at –40°C, indicating sensitivity of toughness to testing temperature — Figs. 9 and 10.

Similar ferritic joints displayed higher CTOD values than the base metal at RT, which can be attributed to the extensive crack tip branching and crack path deviation into the softer base metal due to extremely high overmatching of the fusion zone (about 310%, Table 2) — Fig. 11. The very high CTOD values for similar ferritic laser weld joints are obviously not representing the intrinsic toughness properties of the weld zone, which showed very high hardness values and predominantly bainitic/martensitic microstructure. If the maximum load CTOD values (d_m) are reported (as standard CTOD procedure requires) the toughness level of laser welds will therefore be overestimated. This is due to the effect of lower strength base metal present near the vicinity of the crack tip (laser weld width being approximately 2 mm), which relaxes the stress state at the fatigue crack tip in the middle of the laser weld. The applied deformation principally goes to the lower strength base metal part of the specimen, and hence, the critical fracture stress for a possible brittle fracture at the crack tip cannot be

Table 2 — Summary of the Mechanical Properties of the Laser Beam Welded Joints

	St 37-St 37		St37-Aus		Aus-Aus	
	YS (MPa)	TS (MPa)	YS (MPa)	TS (MPa)	YS (MPa)	TS (MPa)
	230	370	330	419		
	215 (222)	376 (372)	327 (325)	404 (415)	—	—
BM-F	215	367	334	440		
	228	374	307	398		
			326	593	316	611
	—	—	304 (319)	573 (598)	326 (319)	609 (607)
BM-A			320	608	318	601
			325	616	316	607
	640	825				
	730 (685)	893 (851)	900	988	360	552
WM	638	804	580 (740)	606 (797)		
	732	880				
	320	432	416	496		
HAZ-F	316	435	378	472	—	—
	298	421	718	823		
	280	406				
			424	591	448	621
HAZ-A	—	—	410	613	430	619
M(a)	3.09		2.28		1.13	

(a) $M = YS_{wm}/YS_{BM}$

In parentheses, average values are presented for base metals and weld metals.

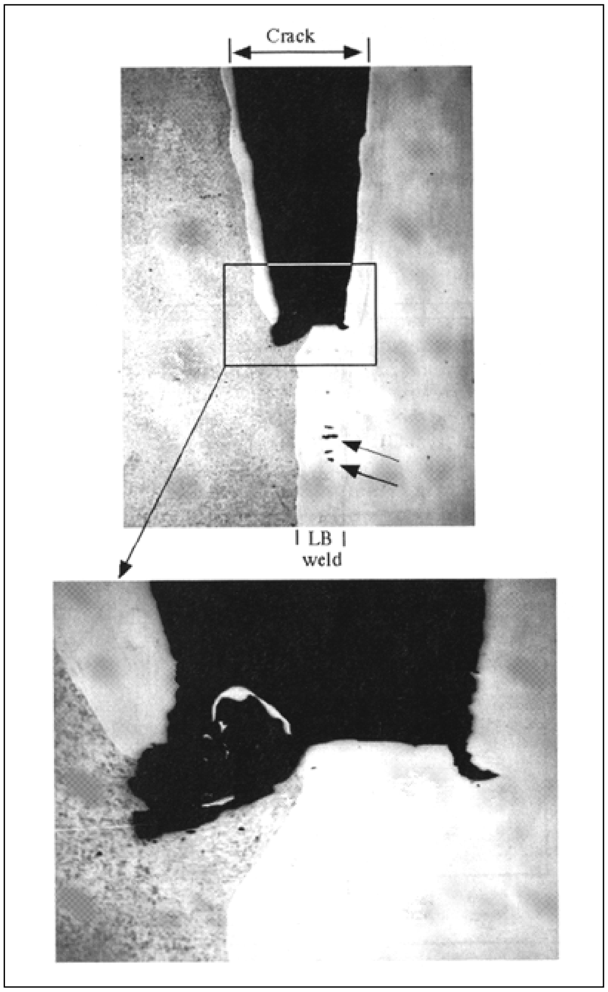

Fig. 12 — Crack propagation in dissimilar joint along the weld zone (small arrows indicating solidification cracks). Note crack path deviation into lower strength ferritic base metal.

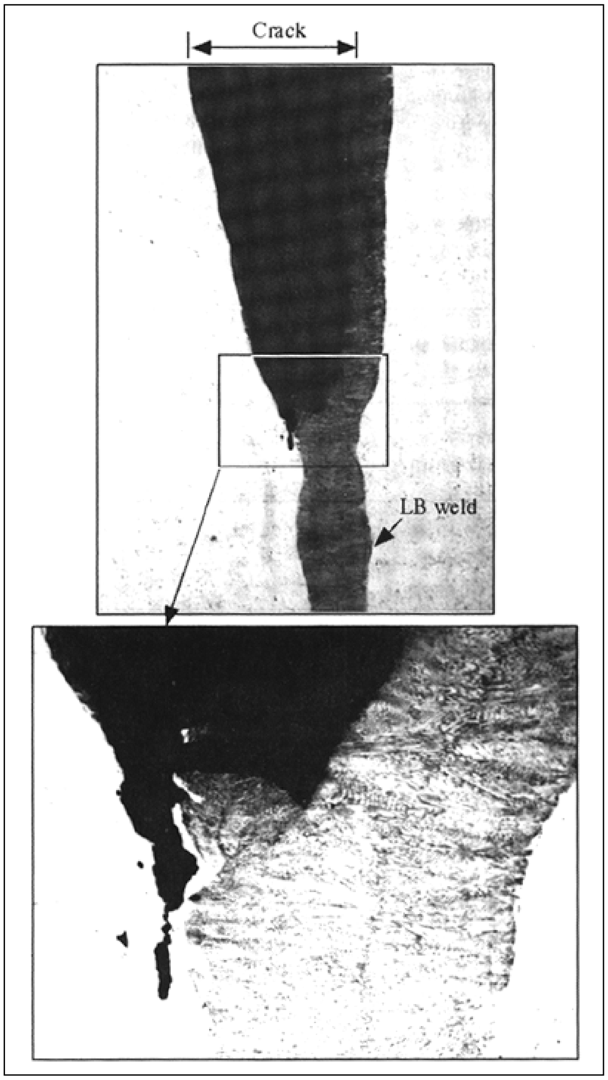

Fig. 13 — Crack propagation in a similar austenitic joint. There is no distinct crack path deviation but the crack propagates in the base metal along the weld zone.

reached for ferritic similar welds.

Dissimilar joints showed the lowest CTOD values at RT (Fig. 9) due to asymmetric plastic zone development, which comes from the strength mismatch between ferritic and austenitic steel base metals (M = 0.76, Table 1). Figure 12 shows the dissimilar joint crack tip that displays a one-sided deformation, and hence, crack growth towards lower strength ferritic steel (the mismatch between the ferritic base metal and fusion zone is about 230%, Table 2). It is interesting to note that the presence of small solidification cracks lying perpendicular to the crack direction in the weld zone of dissimilar joints (Fig. 12) did not show any detrimental effect on the fracture toughness values, although dissimilar joints exhibited slightly lower CTOD values than similar joints. This can be due to the fact that extensive plastic deformation developed at the lower strength ferritic steel side of the specimen (shielding effect of the overmatched weld zone).

Examination of the fracture surfaces as well as the sectioned specimens of similar austenitic welds after testing at RT exhibited no crack tip branching but still a slight crack path deviation into the base metal (overmatching of the fusion zone is about 110%, Table 2) in the austenitic similar joints. The crack propagates along the weld region parallel to the weld at both testing temperatures (Fig. 13) illustrating that these specimens do not contain strength mismatch between the laser weld zone and the austenitic base metal as hardness results indicated. In the dissimilar ferritic-austenitic joints, the crack path deviates clearly into the lower strength ferritic steel side and propagates within the ferritic steel at both testing temperatures as illustrated in Fig. 12. On the other hand, an excessive crack tip branching in the similar ferritic joints was observed, and the cracks always deviated into the softer base metal due to extensive plastic zone development within the base metal at both testing temperatures — Fig. 11.

The fracture behavior of all these specimens can be explained with the help of strength mismatch information, hardness profiles and the microstructures developed in the weld regions. Obviously, the ferritic base metal is the weakest constituent (in terms of tensile strength) in similar ferritic joints and in dissimilar joints into which the crack deviates. This crack path deviation into the lower strength base metal, which is schematically shown in Fig. 14, during standard three-point bend tests with the notch in the overmatched narrow laser weld zone leads to an experimental difficulty in determining the intrinsic fracture toughness properties of thin section C-Mn steel laser welds.

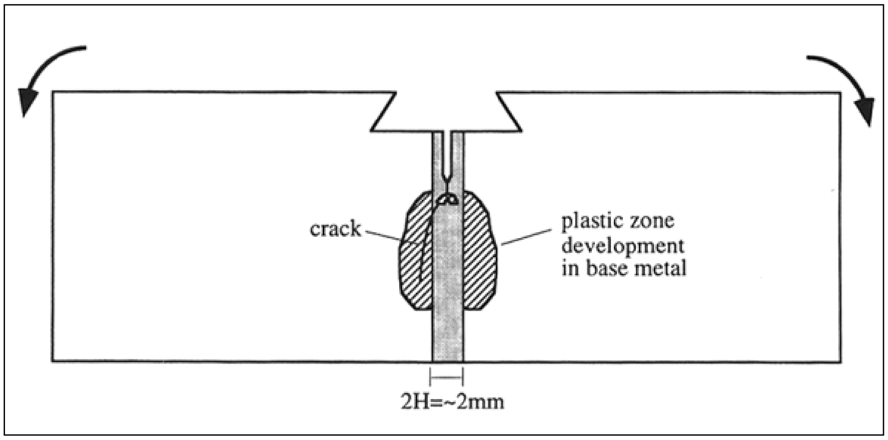

Fig. 14 — Schematic showing extensive plastic zone development in the soft base metal of similar ferritic steel laser beam weld during fracture toughness testing. The crack path deviation inevitably occurs towards the lower strength base metal and the toughness result obtained represents the base metal in thin section laser welds of C-Mn steels.

Conclusions

The results of this work provide the following conclusions:

1) The microstructures of CO_2 laser welded C-Mn steel contain large proportions of bainite/martensite in the weld region due to rapid cooling involved. An extreme hardness increase in the weld regions of ferritic similar joints and ferritic-austenitic dissimilar joints were observed, while there is no significant hardness increase in the weld region of the austenitic steel similar joints.

2) All the transverse tensile specimens of the joints containing ferritic constituent failed at the lower strength ferritic base metal sides due to the strength mismatch effect. Even the presence of some solidification cracks in dissimilar joints did not change the fracture location, due

to the strength overmatching of the weld region.

3) Microtensile specimens extracted from the weld metal of similar ferritic joints displayed significantly higher strength values (M = ~3.1) and markedly lower strain values than the base metal specimens, due to the presence of bainite/martensite in the weld zone. The all-HAZ specimens also exhibited higher strength values and lower strain values than those of the base metal.

4) Similar austenitic joints exhibited no significant property variation across the weld zone as indicated by a hardness profile. The microtensile specimens extracted from the weld zone of the dissimilar joint exhibited high strength and low strain values. The all-HAZ specimens extracted from the HAZ at the ferritic side also displayed higher strength and lower strain values than the ferritic base metal.

5) CTOD fracture toughness testing does not provide "intrinsic toughness value" for thin section laser beam welds owing to crack tip branching and/or crack path deviation towards the lower strength base metal side (mismatch).

6) The CTOD values obtained for similar and dissimilar joints demostrate the toughness trends, which can be explained with strength mismatch and microstructure aspects.

7) Finally, an application of the flat microtensile specimen technique to laser welded joints was demonstrated. By using this technique, it is possible to determine the local mechanical properties of the joints, which can be correlated to the respective microstructure and hardness.

Acknowledgments

This work is a part of the German-Turkish joint project financed by International Bureau, KFA-Jülich and Türkiye Bilimsel Teknik Arastirma Kurumu (TÜBITAK), Turkey. The authors would like to thank both organizations for their financial support. They also would like to thank Mr. S. Riekehr and Mr. H. Mackel for their technical assistance in testing.

References

1. Rippl, P. 1994. Laser beam welding with robots in the automotive industry. *5th European Conference on Laser Treatment of Materials, ECLAT'94*, pp. 151–164, Bremen, Germany.

2. Yeni, Ç., Erim, S., Çam, G., and Koçak, M. 1996. Microstructural features and fracture behaviour of laser welded similar and dissimilar steel joints. *Int. Welding Technology '96 Symposium*, pp. 235–247, Istanbul, Turkey, Gedik Education Foundation.

3. Çam, G., Riekehr, S., and Koçak, M. 1997. Determination of mechanical properties of laser welded steel joints with microtensile specimens. *The ASM International European Conference on Welding and Joining Science and Technology*, pp. 63–79, Madrid, Spain, ASM International, IIW Doc. SC X-F-055-97.

4. Çam, G., Yeni, Ç., Erim, S., Ventzke, V., and Koçak, M. 1998. Investigation into properties of laser welded similar and dissimilar steel joints. *Journal of Science and Technology of Welding and Joining* 3(3).

5. Brown, P. M., and Bird, J. 1996. The laser welding of Q1N, HSLA80 and NSS550. IIW Doc. IX-679-96

6. Kristensen, J. K., and Borgreen, K. 1994. Mechanical properties and microstructures of laser welded constructional steels. *5th European Conference on Laser Treatment of Materials, ECLAT'94,* pp. 226–239, Bremen, Germany.

7. Sun, Z., and Moisio, T. 1994. Effect of processing parameters on laser welded dissimilar joints. *Welding Journal* 73(4): 63-s to 70-s.

8. Strychor, R., Moon, D. W., and Metzbower, E. A. 1984. Microstructure of ASTM A-36 steel laser beam weldments. *JOM*, pp. 59–61

9. Metzbower, E. A. 1990. Laser beam welding: thermal profiles and HAZ hardness. *Welding Journal* 69(7): 272-s to 278-s.

10. Dilthey, U., Dobner, M., Ghandehari, A., Lüder, F., and Träger, G. 1996. Entwicklung, Stand und Perspektiven der Strahltechnik, pp. 1–14, Konferenz Strahltechnik, Halle, Germany.

11. Kalla, G., Funk, M., *et al.* 1993. Heavy section laser beam welding of fine-grained structural steels. *LASER Technology and Applications*, pp. 319, H. Kohler (ed.), Vulkan-Verlag, Essen, Germany.

12. Koçak, M., and Junghans, E. 1994. Fracture toughness properties of similar and dissimilar electron beam welds. *2nd European Conference on Joining Technology*, Florence, Italy.

13. Koçak, M. and Schwalbe, K.-H. 1994. Fracture of weld joints: mismatch effect. Neuentwicklungen im Konstruktiven Ingenieurbau, pp. 137–155, Ed. H. Saal and Ö. Bucak, Univ. of Karlsruhe, Germany.

14. Schwalbe, K.-H., and Koçak, M. 1992. Fracture mechanics of weldments-properties and applications to components. *3rd Int. Conf. on Trends in Welding Research,* pp. 479–494, Gatlinburgh, Tenn.

15. Koçak, M., Es-Souni, M., Chen, L., and Schwalbe, K.-H. 1989. Microstructure and weld metal matching effects on heat affected zone toughness. *8th Int. Conf. OMAE-ASME*, pp. 623–633, The Hague, Netherlands.

16. Kirk, M. T., and Doods, R. H. 1992. The influence of weld strength mis-match on crack tip constraint in single edge notch bend specimens. University of Illinois Report, UILU-ENG-92-2005.

17. Cao, H. C. and Evans, A. G. 1994. An experimental study of the fracture resistance of bi-material interfaces. *Mechanics of Materials* 7: 295–304.

18. Kristensen, J. K. 1996. Procedure qualification, process monitoring, NDT and adaptive welding control. *Int. Conf. on Explotation of Laser Processing in Shipyards and Structural Steelworks*, Glasgow, U.K.

19. Klausnitzer, E. 1976. Entwicklung eines Verfahrens zur Entnahme und Prüfung von Mikro-Flachzugproben aus der WEZ von Schweißverbindungen. *Materialprüfung* 18(11): 411–416

20. Çam, G., Bohm, K.-H., Müllauer, J., and Koçak, M. 1996. The fracture behavior of diffusion-bonded duplex gamma TiAl. *JOM*, pp. 66–68.

21. Çam, G., Müllauer, J., and Koçak, M. 1997. Diffusion bonding of two-phase g-TiAl alloys with duplex microstructure. *Journal of Science and Technology of Welding and Joining* 2(5): 213–219.

22. Koçak, M., and Denys, R. 1994. CTOD and wide plate testing of welds with particular emphasis on mis-match welded joints. *10th European Conf. on Fracture, ECF 10, Structural Integrity, Experiments, Models, Applications,* pp. 97–120, Edited by K.-H. Schwalbe and C. Berger, Engineering Materials Advisory Services (EMAS) Ltd.